BEYOND THE FOCAL LINE: RE-DESIGNING PARABOLIC TROUGHS FOR RECEIVER LONGEVITY

Summary

The research aims to improve the reliability of the receiver tube in the LS-III Parabolic Trough Collector (PTC) through a novel design that splits the common focal line into two lateral foci and lowers the receiver relative to the geometric focus. This split-focus, shifted-receiver layout spreads the incident flux, cuts peak intensities, and reduces circumferential gradients that drive thermal stress. A well-established Monte Carlo Ray Tracing (MCRT)-based Optical Design Optimization (ODO) approach is used to statistically evaluate various geometries across multi-parametric combinations. The results show clear trade-offs: while optical efficiency drops by ~5–6% relative to the benchmark LS-III, flux uniformity index (*U*) improves, and peak flux is substantially reduced. The study indicates that modest geometric changes can maintain acceptable efficiency, improve off-sun robustness, and suppress hotspots. Hence, potentially extends the receiver's lifespan and reduces maintenance and replacement costs in solar thermal power plants.

Keywords: Flux distribution, MCRT, Optical design optimization, parabolic trough collector, receiver tube.

Field of application for the findings: Concentrating Solar Power (CSP) and Solar Thermal Power Plants

Addressed audience: Solar engineers, researchers, and plant operators interested in component reliability.

1. Introduction

PTCs are the most widely deployed line-focus CSP technology, valued for their scalability and compatibility with thermal storage. However, the conventional single-focus layout, with the receiver centered at the geometric focus, heightens sensitivity to tracking and figure errors and produces strongly peaked, circumferentially uneven flux on the tube. Resulting hot spots intensify thermal gradients, accelerate coating and glass envelope degradation, and shorten receiver life, increasing maintenance demands. Earlier performance enhancement attempts, such as secondary reflectors, larger rim angles, changes in receiver diameter, and location, are reported but largely preserved the single-focus model and did not prioritize flux uniformity as a primary design target.

This research is a pilot study on improving the base LS-III PTC with a novel design that splits the aperture into two symmetric parabolic segments with laterally separated foci and lowers the receiver relative to the geometric focus. This approach relaxes tracking precision by allowing rays to concentrate on two points rather than a single common focus. Hence, ultimately increases the receiver surface area exposed to solar rays, significantly flattens the peak flux, and consequently minimizes the risk of hotspot formation. An MCRT-based ODO explores receiver height, focus shift, and incidence angle, and evaluates designs using optical efficiency and reliability-relevant metrics, such as the uniformity index and peak flux reduction. Findings indicate that modest geometric changes can retain efficiency within a narrow penalty window and markedly improve flux uniformity, suggesting a practical route to longer receiver life and stable field operation.

2. PTC Geometry and Materials

2.1. Geometric details

Fig. 1 contrasts the baseline LS-III trough (Fig. 1a) (Zou et al., 2019) with the modified configuration (Fig. 1b), along with the corresponding geometry and parameter set used for optical simulation. The modified design divides the aperture into two symmetric parabolic segments whose focal points are laterally displaced by a horizontal offset d_x about the collector's vertical axis. To preserve the optical aperture, the segmentation and focal shift are dimensioned to maintain a clear aperture width of $W = 5760$ mm.

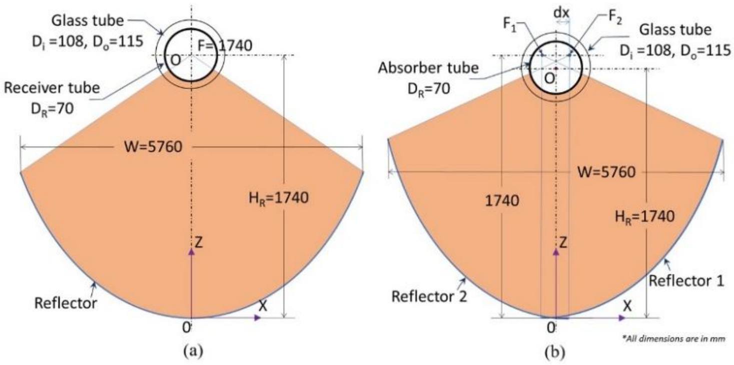

Fig. 1: Geometry of PTC: (a) base LS-III design, (b) concept of horizontal split-focus with receiver vertical-shift

2.2. Optical materials

The study uses advanced, wavelength-dependent materials listed in Tab.1, which are used in next-generation solar collectors. The receiver is enclosed in an evacuated glass tube coated with an anti-reflective coating.

Tab. 1: Wavelength-dependent optical materials used for simulation, Leal et al. (2024)

Part	Material name	Description
Reflector (collector)	Silver-Glass (Ag)	4 mm water-white glass with silver layer (scattering error due to the specular reflectance is considered)
Absorber (receiver)	TiAlN-TiAlON-Si_3N_4	Thin film on metallic absorber
Glass tube	SiO_2	3.5 mm thick glass tube
Anti-reflective coating	MgF_2	Thin film on inner and outer surfaces of glass tube

3. Methodology

Parametric geometries were built in FreeCAD and exported to OTSunApp for a two-stage MCRT–ODO. The simulations are performed with a circumsolar ratio (CSR) = 0.05 using the Buie sunshape model. The modified design (Fig. 1b), H_R, and d_x are varied as per Tab. 2, while the remaining specifications are held constant. A total of 328 geometric combinations is obtained and simulated with the incidence angle, θ, from 0° to 2° in steps of 0.25°, yielding 2952 cases. The First stage of MCRT-ODO is simulated using the Total analysis module of OTSunApp. The geometries with higher optical efficiencies (η_o) are filtered and processed for the second stage, which is performed using the Spectral analysis module of OTSunApp. Here, the circumferential flux and local concentration ratio (LCR) on the receiver surface are computed. The flux distribution is evaluated via statistical metrics like Coefficient of Variation (CV) (ratio of standard deviation, σ_{LCR} to average, μ_{LCR}), uniformity index (U), and scored with a weighted objective function (S) with weightages w_1 and w_2.

$$U_{LCR} = \frac{1}{1+CV} \quad \text{(eq. 1)}$$

$$\text{Flux Uniformity Increase, } \Delta U_{\text{LCR}} = \left(\frac{U_{\text{new}} - U_{\text{baseline}}}{U_{\text{baseline}}}\right)_{LCR} \times 100 \quad \text{(eq. 2)}$$

$$\text{Peak Flux Reduction, } \Delta R_{peak} = \frac{LCR_{\text{peak,baseline}} - LCR_{\text{peak,new}}}{LCR_{\text{peak,baseline}}} \times 100 \quad \text{(eq. 3)}$$

$$S = w_1 \cdot \Delta U_{\text{LCR}} + w_2 \cdot \Delta R_{\text{peak}} \quad \text{(eq. 4)}$$

Tab. 2: Variable parameters, range, and step for FreeCAD geometry construction.

Parameters	Base values of LS-III	Range for modification (from-to)	Step
Receiver Height (H_R)	1740 mm	1600 to 1800 mm	5 mm
Focal shift distance (d_x)	0 mm	0 to 35 mm	5 mm

4. Results and Conclusion

With high-end optical properties, the reference PTC reaches η_o of 84.5%, while constant-property inputs with the same CSR in base LS-III yield η_o of 78-80% (Zou et al., 2019). As the incidence angle, θ, increases (Fig. 2a), η_o declines for all cases up to $\theta \approx 1°$; beyond this, split-focus designs ($d_x > 0$) retain or exceed the single-focus performance, indicating improved ray capture off-sun. The H_R zones with a 5% window of η_o are highlighted for all θ, and are combinedly shown in Fig. 2(b) for $\theta = 0°$. The cases with high η_o are termed the High-Precision zone, which needs accurate tracking but relaxed up to $\theta = 0.75°$. In contrast, cases that provide stable η_o from 38% to 48% with tracking relaxation up to $\theta = 2°$ are categorized as the High-Tolerance zone.

Spectral analysis of High-Precision candidates highlights three representative heights: $H_R = 1740$, 1725, and 1705. Flux profiles (Fig. 3a and 3b) show that split-focus with lowered H_R flattens peaks and spreads irradiance over a wider circumferential area. The composite score, S with $w_1 = 0.7$ and $w_2 = 0.3$ (Fig. 3c), ranks $H_R = 1725$ highest across relevant shifts, reflecting strong gains in uniformity, U, and substantial peak-flux reduction R_{peak}, with an optical-efficiency penalty of only 5–6% relative to LS-III.

Solar PTC power plants allocate a higher share of costs to receiver reliability and thermal stress mitigation than to marginal gains in optical efficiency. Since non-uniform flux and hotspot formation are leading contributors to receiver degradation and maintenance issues in PTC plants, the proposed geometry provides a net benefit to plant reliability and lifecycle performance.

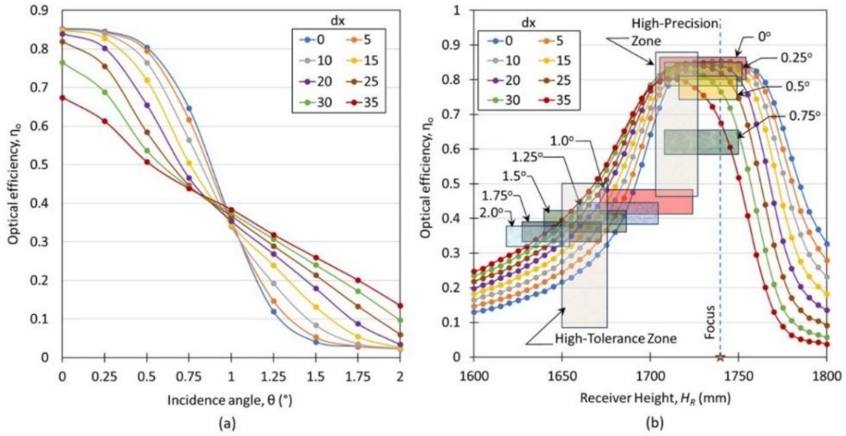

Fig. 2: Effect of split-focus geometry of optical efficiency with varying incidence angle: (a) H_R =focus, (b) variable H_R

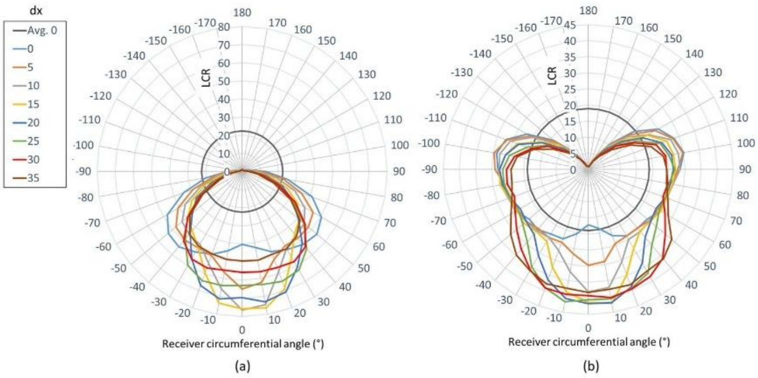

θ=0°		H_R 1740	1725	1705
dx	0	0.0	14.7	35.7
	5	-7.4	14.3	35.6
	10	-16.4	6.4	29.1
	15	-17.8	3.8	25.3
	20	-16.7	2.9	23.7
	25	-11.8	3.5	23.2
	30	-7.7	5.1	23.2
	35	-2.9	6.7	23.8
θ=0.75°				
dx	0	0.0	-2.6	-0.7
	5	-6.1	2.8	3.5
	10	-7.9	3.1	6.9
	15	-2.2	3.5	9.1
	20	2.9	5.9	11.1
	25	5.1	7.0	11.6
	30	6.9	7.5	11.8
	35	9.4	9.4	11.0

(c)

Fig. 3: Flux distribution profile on the receiver circumference at $\theta = 0°$: (a) $H_R = 1740$, (b) $H_R = 1705$, (c) S-values

5. References

Leal, M., Pujol-Nadal, R., Domingo Álvarez, J., del Mar Castilla, M., Torres, J. L., Cardona, G., & Pérez, M., 2024. Optical performance analysis of a hybrid parabolic trough collector with photovoltaic slats. Applied Optics, 63(34), 8878-8889.

Zou, B., Jiang, Y., Yao, Y., & Yang, H., 2019. Optical performance of parabolic trough solar collectors under condition of multiple optical factors. Applied Thermal Engineering, 160, 114070.